Experiments on "above-threshold ionization" of atomic hydrogen

H. G. Muller, H. B. van Linden van den Heuvell, and M. J. van der Wiel
FOM Institute for Atomic and Molecular Physics, Kruislaan 407, 1098 SJ Amsterdam, The Netherlands
(Received 6 January 1986)

The multiphoton ionization of atomic hydrogen is studied by means of photoelectron spectroscopy. The order of nonlinearity of the ionization process via the $3p$ resonance is measured for intensities in the 10^{11}-W/cm^2 range, revealing that the three-photon excitation step is rate limiting. What may be the first measurement on "above-threshold ionization" (ATI) of atomic hydrogen is reported, performed as a function of the real momentary light intensity. Agreement between the measured relative ATI yield and the theoretically predicted one is within 10%. Possibilities to extend the measurements into the regime where perturbation theory breaks down are investigated by means of a two-color experiment.

I. INTRODUCTION

Irradiation of atoms with light of high intensity gives rise to a number of interesting processes, like ionization by absorption of a number of photons simultaneously, where the "intermediate" steps reach either virtual levels in the discrete part of the atomic spectrum [multiphoton ionization (MPI)], real atomic levels [resonance-enhanced MPI (REMPI)], or continuum states of the atom [above-threshold ionization (ATI)]. (See, e.g., Refs. 1 and 2). In this paper the interest is confined to experiments, based on the analysis of photoelectron energies.

Since the generalized cross sections associated with ATI are difficult to calculate because they often depend critically on the level structure of the atom, comparison between experiment and theory has been difficult. For the ATI process, the best results so far have been obtained for the ionization of alkali-metal atoms, notably cesium,[3] where the probability of ATI with one extra photon was computed. In addition to this computational problem, the comparison with experiment is hindered by the fact that in an actual experiment MPI is mostly measured at many intensities simultaneously. Even with detailed knowledge of the laser focus parameters the connection with theory is very indirect at best.[4]

In this paper both problems mentioned above are evaded. The problem of the intensity distribution in a laser focus is solved by the use of "Stark-shift tuning" through an intermediate resonance, to select a particular ionization intensity. This technique was introduced recently in an ATI experiment on xenon.[5,6] However, the case of Xe is obviously more difficult to treat theoretically. Only a lower bound to the first ATI cross section could be calculated, which turned out to underestimate the experimental ATI rate by a factor of 5.[7]

In order to alleviate the computational problems, there is demand for measurements on atoms which can be treated conveniently by theorists, such as atomic hydrogen, for which a large number of calculations have already been performed, even with nonperturbative methods.[8,9] So far only one experiment on atomic hydrogen has been published, in which the four-photon REMPI cross section at $\lambda \approx 364$ nm was measured as a function of light intensity.[10] Despite the fact that the kinetic energy of the released electron is extremely small, a fact which makes the process in principle critically dependent on level shifts, Kelleher *et al.*[10] observe an order of nonlinearity of two for the maximum of the ionization rate. This is in accordance with theory. Here we report a second experiment on atomic hydrogen, in which ATI is studied for the first time to our knowledge.

This type of measurement, and in particular on ATI, is exceedingly difficult, since the ionization cross section of atomic hydrogen is small, and the ionization potential high, requiring the use of energetic photons. Under these circumstances the ATI yield is very low, demanding an energy analyzer of outstanding sensitivity in order to measure the photoelectron spectrum.

At the intensities used in this paper there is no doubt about the correctness of the description of the ATI process by perturbation theory. The theoretical treatment of the process is therefore essentially exact. The aim of this paper is therefore not so much to test theory, but more to show that current experimental techniques do allow quantitative measurements of such elusive processes as ATI.

II. THEORY

Calculations on multiphoton processes in the hydrogen atom have been performed by a number of authors, applying various methods (e.g., Refs. 11–13), which are all in agreement. We also have developed a computer program to calculate matrix elements of multiphoton processes, which works by numerically integrating the wave functions in spherical coordinates, similar to the method of Aymar and Crance. This program reproduces most of the earlier mentioned results, and is described elsewhere.[14] It was used to calculate a number of matrix elements, which are compiled in Tables I and II and which are relevant to either the REMPI process through the $3p$ state, or the two-color processes to be discussed below. These matrix elements are used to calculate the shift of the relevant atomic levels, as well as their decay rate by ionization to different channels. The resulting shift and rates are

TABLE I. Radial integrals for the various matrix elements of the three-photon resonance to $|3p\rangle$. ($\omega_1=0.148\,148$ a.u.) $R_l(E)$ is the projection of the resolvent $(E-H)^{-1}$ on the subspace of angular momentum l. $E_n=E_{1s}+n\omega_1$.

Matrix element	Value (a.u.)	Total
Stark shift		
$\langle 1s \mid zR_p(E_1)z \mid 1s\rangle$	-1.667	-5.18
$\langle 1s \mid zR_p(E_{-1})z \mid 1s\rangle$	-3.515	
$\langle 3p \mid zR_s(E_4)z \mid 3p\rangle$	403.4	49.7
$\langle 3p \mid zR_s(E_2)z \mid 3p\rangle$	-419.5	
$\langle 3p \mid zR_d(E_4)z \mid 3p\rangle$	365.7	
$\langle 3p \mid zR_d(E_2)z \mid 3p\rangle$	-321.3	
Three-photon excitation		
$\langle 1s \mid zR_p(E_1)zR_s(E_2)z \mid 3p\rangle$	-76.41	-107.2
$\langle 1s \mid zR_s(E_1)zR_d(E_2)z \mid 3p\rangle$	-30.76	
One-photon ionization		
$\langle 3p \mid z \mid E_4s\rangle$	0.551	
$\langle 3p \mid z \mid E_4d\rangle$	1.116	
Two-photon ionization (ATI)		
$\langle 3p \mid zR_s(E_4)z \mid E_5p\rangle$	$-11.24+14.69i$	$-0.77+19.67i$
$\langle 3p \mid zR_d(E_4)z \mid E_5p\rangle$	$10.46+4.98i$	
$\langle 3p \mid zR_d(E_4)z \mid E_5f\rangle$	$-11.56+14.05i$	

shown in Table III. Within the framework of perturbation theory, no other approximations are made in calculating the matrix elements. The physical quantities in Table III, however, are calculated from these matrix elements under rather idealized assumptions of zero bandwidth and lowest-order perturbation theory. For the experiment at hand these assumptions are expected to be quite good.

III. EXPERIMENTAL SETUP

Atomic hydrogen was produced by means of a microwave discharge in a 2.4-GHz cavity. The input power into the microwave cavity was around 100 W. Hydrogen gas was led through the cavity, at a pressure of ≈ 100 Pa, by means of an aluminum oxide tube coated with boric acid. The mixture of H and H_2 so produced, expanded through a 1-mm-diam orifice into the ionization chamber, where it was ionized by means of a laser beam, focused by a plane-convex fused-silica lens of 25-mm focal length. The atomic hydrogen pressure in the ionization chamber was estimated to be 10^{-2} Pa. By observing an MPI signal due to H_2 molecules with the discharge switched on and off, it was established that 40% of the molecules were dissociated into atoms. This low value is not due to inefficiency of the source itself, but rather to the inefficient pumping of the ionization chamber, giving the H atoms

TABLE II. Multiphoton matrix elements for various pathways. R_{nm} means the resolvent operator $(E_{nm}-H)^{-1}$, taken at energy $E_{nm}=E_{1s}+n\omega_1+m\omega_2$. $\omega_1=0.16$ a.u. (285 nm), $\omega_2=0.042\,828$ a.u. (1064 nm).

Matrix element	Value
Five-photon ionization pathways	
$\langle 1s \mid zR_{10}zR_{20}zR_{21}zR_{22}z \mid E_{32}p\rangle$	10.5×10^{6}
$\langle 1s \mid zR_{10}zR_{20}zR_{21}zR_{22}z \mid E_{32}f\rangle$	6.99×10^{6}
$\langle 1s \mid zR_{10}zR_{20}zR_{21}zR_{22}z \mid E_{32}h\rangle$	4.64×10^{5}
Five-photon ATI pathways	
$\langle 1s \mid zR_{10}zR_{20}zR_{21}zR_{31}z \mid E_{32}p\rangle$	$-5.52\times10^{6}-13.1\times10^{6}i$
$\langle 1s \mid zR_{10}zR_{20}zR_{21}zR_{31}z \mid E_{32}f\rangle$	$7.59\times10^{6}-13.7\times10^{6}i$
$\langle 1s \mid zR_{10}zR_{20}zR_{21}zR_{31}z \mid E_{32}h\rangle$	$2.86\times10^{6}-1.04\times10^{6}i$
Four-photon ionization pathways	
$\langle 1s \mid zR_{10}zR_{20}zR_{21}z \mid E_{31}s\rangle$	-4.01×10^{4}
$\langle 1s \mid zR_{10}zR_{20}zR_{21}z \mid E_{31}d\rangle$	-8.63×10^{4}
$\langle 1s \mid zR_{10}zR_{20}zR_{21}z \mid E_{31}g\rangle$	-1.26×10^{4}

TABLE III. Some quantities relevant to the REMPI process at $\omega_1 = 307.6$ nm.

Ionization rate from $3p$ with 1 uv:	2.866×10^{9} $s^{-1}/(GW/cm^2)$
Ionization rate from $3p$ with 2 uv:	9.472×10^{3} $s^{-1}/(GW/cm^2)^2$
Ionization rate from $3p$ with 2 ir:	1.34×10^{8} $s^{-1}/(GW/cm^2)^2$
Stark shift of $1s\rightarrow3p$ by uv:	0.54×10^{-3} $nm/(GW/cm^2)$
Stark shift of $1s\rightarrow3p$ by ir:	7.64×10^{-3} $nm/(GW/cm^2)$
Excitation rate $1s\rightarrow3p$ by uv:	1.079×10^{-3} $s^{-1}/(GW/cm^2)^3$

ample time to recombine on the walls of the apparatus. Most of our measurements, however, are not disturbed by the presence of the molecules, since these are much harder to ionize. For reasons of diagnostics, the entire experiment was conducted with deuterium as target gas. We assume that the choice between hydrogen and deuterium is of no relevance for the process studied here.

In the experiments in which two beams of different color were used, a second laser beam entered the ionization chamber from the other side, focused by a lens of 50-mm focal length. A good overlap of the focal regions was obtained by adjusting the lenses while monitoring the signals due to absorption of photons from both beams by xenon gas.[15] The uv radation used was obtained by frequency doubling the output of a dye laser (linewidth 3 GHz), pumped with the second harmonic of a Nd:YAG laser (where YAG denotes yttrium aluminum garnet). Pulses obtained from this laser system have a typical duration of 6 ns, and energies of 300 μJ. This energy and pulse width correspond to a peak intensity of 10^{11} W/cm^2. The pulse energy of the uv beam was measured by splitting off a tiny part of the laser beam and directing it to a photodiode. The energy E of every laser pulse was recorded simultaneously with the measurement of the yield of MPI electrons. This enabled the recording of the photoelectron signal as a function of pulse energy over the range of random fluctuation of the laser pulse. Since this range was rather small, this empirical dependence could conveniently be fitted by a straight line. This line was then used to determine the photoelectron signal at a standard energy, eliminating the random pulse-energy fluctuations as a source of noise from our data. Note that this procedure corrects for pulse energy, and not for intensity fluctuations. The order of nonlinearity need not be assumed in order to perform this correction, and in fact does not have any influence on the energy-signal relationship. (See Sec. IV A). For scans over a broad range of pulse energies, at constant wavelength, use was made of a double Fresnel rhomb to rotate the plane of polarization, followed by a polarizer in the uv beam. This method of energy variation is known to preserve beam shape, and therefore focal parameters, very well.[5]

The electrons produced by the various MPI processes were time-of-flight (TOF) analyzed in our 2π spectrometer[16] and detected on a double channel plate in a chevron mount. For each laser shot, the analog signal from the channel plates, i.e., the total charge in each pulse, was digitized in a storage oscilloscope, and stored in the memory of a microcomputer for further processing.

In order to compare the yield of processes that differ vastly in cross section, the amplification of the channel plates was changed by adjusting the voltage across them. In order to preclude pressure-dependence effects, a relative calibration of the amplification as a function of voltage was made under identical circumstances as the experiment itself. This was done by comparing step by step the photoelectron signal at two different voltages across the channel plates, in a situation with a constant photoelectron production. Whenever two measurements at different setting of the voltage were necessary, care was taken in order to perform them immediately after one another (usually within 2 min), to avoid a possible change in shape of the focal spot due to uncontrollable parameters like degradation of the laser dye or conditions of the microwave discharge. Therefore the only difference between two

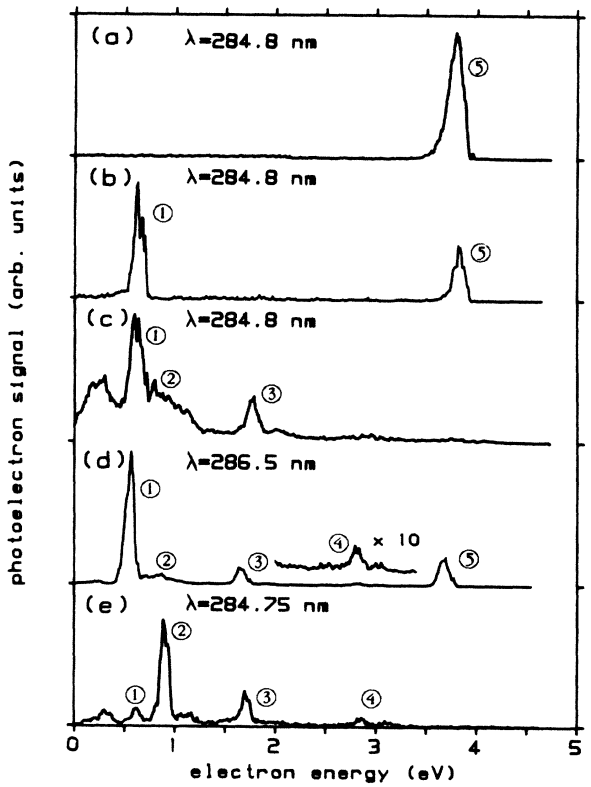

FIG. 1. The electron energy spectrum at various wavelengths, for ionization with uv and ir. (a), (b), and (c) are taken at the top of the $5p/5f$ Stark-broadened resonance profile of Fig. 7, with increasing ir intensity. Similarly (d) is taken near the top of $3p$. (e) is taken at the short-wavelength side of the $5p/5f$ resonance.

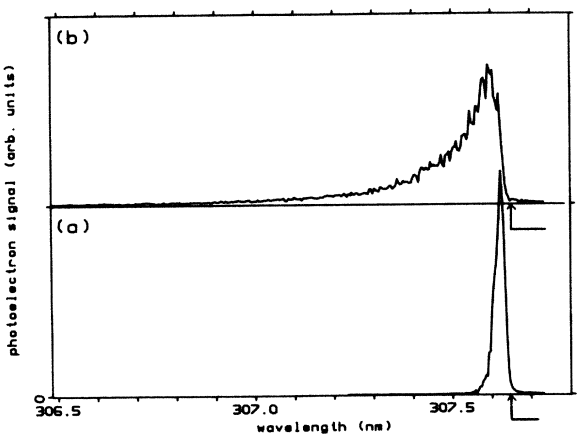

FIG. 2. Photoelectron signal as a function of wavelength in a four-photon MPI experiment. (a) without, and (b) with 1.064 μm radiation present. The high infrared intensity (and to a lesser extent the ultraviolet) causes the resonance to shift away from its weak-field position, indicated by the arrow. The fact that no resonant enhancement is found at the long-wavelength side of this position is experimental evidence for the fact that the shift is large compared to the broadening.

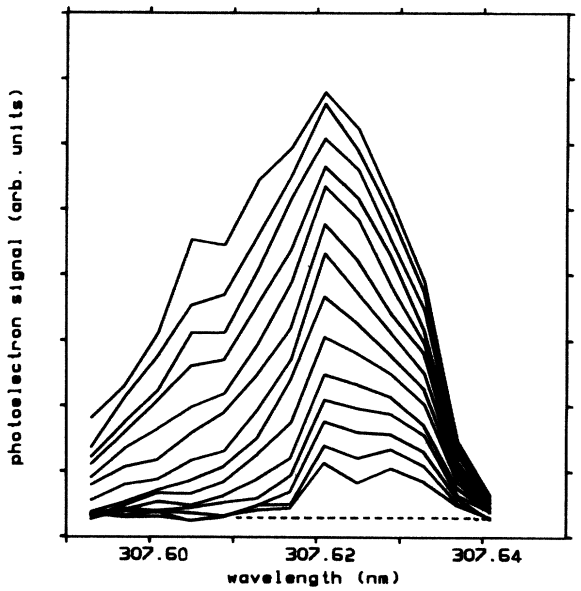

FIG. 3. The resonance profile for laser pulses of different energies. From the lowest to the highest curve these energies are 61, 67, 73, 79, 85, 90, 96, 102, 108, 114, 120, 125, 131, and 137 μJ. The profiles at the highest energies seem to extend to wavelengths shorter than 307.59 nm. No correction for this missing tail was made when calculating the order of nonlinearity, but the background (dashed line) was subtracted.

such measurements should be the random variations of pulse energy due to multimode interference, which is largely corrected for, and the detector which was calibrated to within 10%.

The results of the experiment, given in the following section, are mainly presented in the form of either one of two types of scans:

(i) An energy scan obtained from converting a TOF measurement of the photoelectrons to an energy scale, measured at a constant wavelength. (An example is Fig. 1.)

(ii) The integrated peak area of one of the peaks of a TOF spectrum, measured as a function of wavelength. (An example is Fig. 2.) So when in the following we refer to the yield of electrons of a certain energy, in fact an energy band wide enough to allow for the small spread in energy around this value is meant, thus making the quoted values insensitive to changes of this spread. (Such changes are, for instance, caused by the variation of energy resolution with signal due to space-charge effects.)

IV. RESULTS OF 308 nm

A. Four-photon REMPI through the $3p$ state

When exciting the H atoms with light of a wavelength in the neighborhood of 307.5 nm, a REMPI process occurs, in which three photons excite the atom from its $1s$ ground state to the $3p$ state, followed by ionization with one photon, yielding electrons of 2.5 eV. With our linearly polarized light, the $3p$ state is the only one of the degenerate set $3s$, $3p$, and $3d$ that can be resonantly excited. A measurement of the production of 2.5-eV photoelectrons, as a function of wavelength, is shown in Fig. 2(a).

The variation of the 2.5-eV signal with pulse energy was measured at each wavelength, and the resulting data is compiled in Fig. 3, where the resonance profile for a number of different pulse energies is plotted. The area under the various profiles grows with pulse energy according to a power law, as shown in Fig. 4. The exponent of

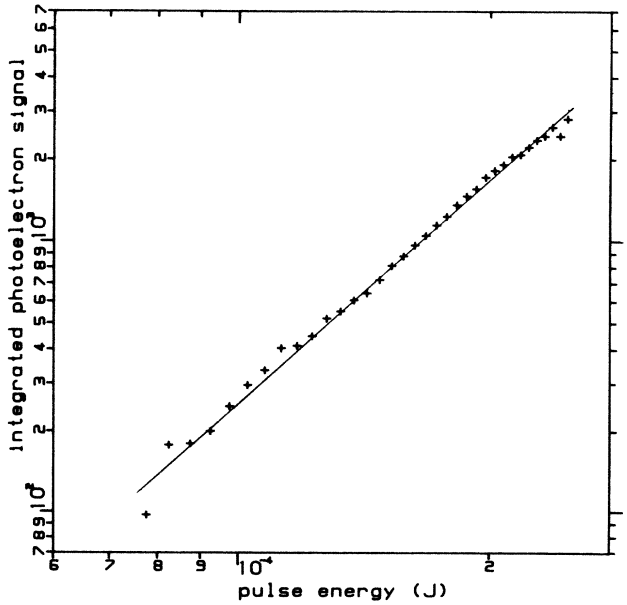

FIG. 4. The ionization signal integrated over wavelength as a function of pulse energy. The line corresponds to an order of nonlinearity of 2.8.

this power law was determined from a least-squares fit to be 2.8 ± 0.1. The intensity of the ionizing radiation shifts (ac Stark shift) as well as broadens (lifetime broadening) the resonance profile, resulting in the usual asymmetric line shape.[5] In the case where ionization with one photon is possible, shift and broadening have the same dependence on intensity (namely a simple proportionality), so their ratio is an atomic constant. Our calculations (see Table III for the relevant numbers) predict the shift to be 11 times larger than the broadening, and the experimentally observed asymmetry indeed confirms that the shift is the dominant broadening mechanism. Otherwise the profile would extend to the other side of the low-field resonance position as well. This situation is in marked contrast with that in the resonant process via the $2p$ state, studied by Kelleher *et al.*,[10] where shift and broadening are about equal. Because of the large ratio, in our case the ionization rate R_I at intensity I can conveniently be approximated by

$$R_I(\lambda)=\sigma I^N\delta[(\lambda-\lambda_0)-\alpha I]\ , \tag{4.1}$$

where αI represents the ac Stark shift. The signal $S_E(\lambda)$ measured at one specific λ during a pulse of energy E is the integral of $R_I(\lambda)$ over all intensities present in the focus, weighed by a normalized distribution function $P_E(I)$ in a pulse of energy E, $P_E(I)$:

$$S_E(\lambda)=\int P_E(I)R_I(\lambda)dI\ . \tag{4.2}$$

As already remarked by Kruit *et al.*,[5] the dependence of $S_E(\lambda)$ on E contains no information on R_I at all, but instead depends critically on P_E. Putting (4.1) in (4.2) and integrating over λ we obtain a quantity proportional to the expected value of I^N, and proportional to E^N as well, if the intensity in every point of the focus scales with E. The slope of the line in Fig. 4 therefore gives the order of nonlinearity N for the process.

Our results as well as that of Kelleher *et al.*[10] confirm that in a resonant multiphoton ionization process the step in which the largest number of photons participate becomes rate-limiting, the order of nonlinearity of the total process becoming equal to this number of photons. The fact that our measured value of N is somewhat on the low side is not very disturbing, since a number of reasons could be invoked that lower the measured value of this quantity, for instance saturation due to ground-state depletion at the highest energies.

B. Above-threshold ionization (ATI)

If the wavelength differs appreciably from the one needed for resonance, no signal is recorded, which implies that ionization through nonresonant processes in negligible. As mentioned in Sec. IV A the high intensity needed for MPI shifts as well as broadens the resonance profile; the equation for R_I, described there, shows how the profile reflects the intensity distribution in the laser focus.[5] The fact that the width due to lifetime reduction and laser linewidth both turn out to be small compared to the ac Stark shift of the $3p$ state, imply that the conditions for ac-Stark-shift tuning are met:[5] If a signal is obtained at a wavelength differing by $\Delta\lambda$ from the zero-field resonance wavelength λ_0, the signal must have been created at a position in the focus where the momentary intensity I was such as to bring the intermediate level into resonance by ac Stark shift. $\Delta\lambda$ and I are coupled by $\Delta\lambda=\alpha I$, where α is the ac-Stark-shift coefficient. An additional requirement for Stark tuning is of course that the ionization takes place in a time that is short compared to the time scale in which the intensity of the laser can vary. The latter is essentially the inverse of the linewidth of the laser. This requirement is clearly fulfilled in our experiment since the linewidth of the laser is around 3 GHz, which is several orders of magnitude less than the expected rate of one-photon ionization out of the $3p$ state. Under these conditions the wavelength scale also represents an intensity scale; this offers the possibility to study the ATI event as a function of well-defined intensity, which is also known absolutely since α is known from Table III.

In Fig. 5 an example of an ATI electron-energy peak is given. The initial energy of the electrons after absorption of one additional photon is 6.5 eV. During the measurement we suppress the four-photon, 2.5-eV electrons by applying a decelerating electric field of 4 V in the TOF tube. This was done in order to avoid detector saturation, because the 2.5-eV signal is about four orders of magnitude larger than that due to the ATI electrons. Therefore it has to be measured in a separate run with a different setting of the channel-plate voltage. The ratio of the five- to the four-photon peak (corrected for variation of laser energy between runs) is shown in Fig. 6, and is proportional to the detuning, i.e., intensity as is predicted by perturbation theory for this energy regime.

The ratio of five- and four-photon ionization is calculated to be 3.305×10^{-6} $(\mathrm{GW/cm^2})^{-1}$, as can be deduced from Table III. The individual data points scatter around the theoretical line with an average deviation of 10%. A least-squares fit of a line constrained to go through zero at

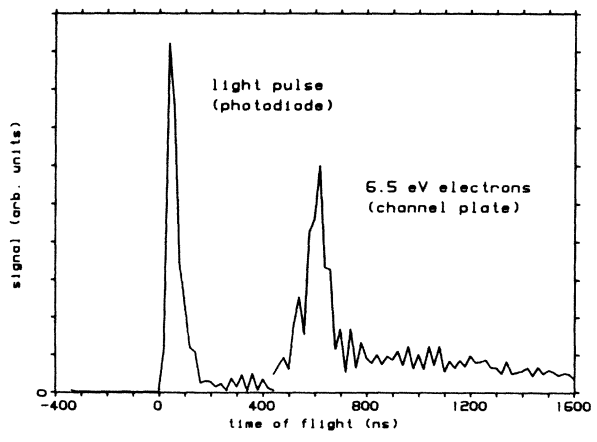

FIG. 5. Time-of-flight spectrum at the top of the resonance in Fig. 2(a). A retarding voltage of 4 V blocks all electrons produced by four-photon MPI. The position of the electron peak corresponds to 6.5-eV electrons, produced in the ATI process.

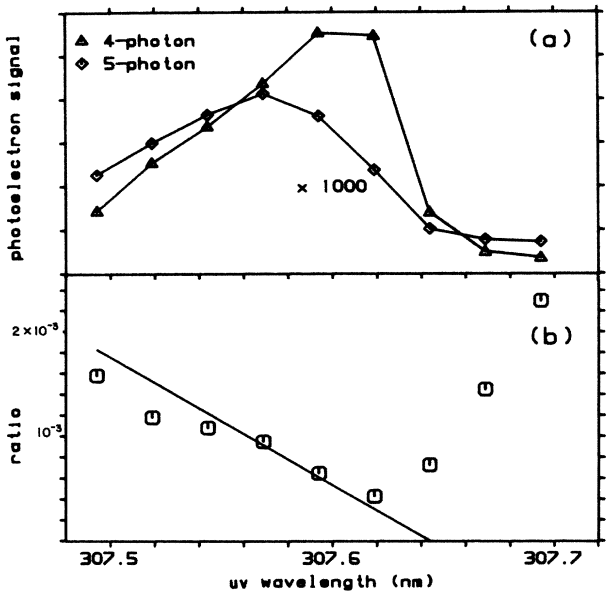

FIG. 6. Branching ratio between four- and five-photon MPI. The resonance profiles for the individual processes (energy peaks at 2.5 and 6.5 eV) are shown in (a), while in (b) the ratio of the two processes is given as a function of wavelength. The line drawn in (b) is the theoretical expectation.

the resonance position leads to a value of 3.12×10^{-6} $(\mathrm{GW/cm^2})^{-1}$. This deviates only 5% from the theoretical value. This is a remarkable close agreement if one considers that the five-photon ionization rate is 3 orders of magnitude smaller than the four-photon ionization rate in this experiment.

The fact that the ratio again rises sharply at the long-wavelength side of the resonance, can be understood easily. Obviously the mechanism of intensity selection does not operate there, many intensities (including the high ones) contributing to the ionization, increasing the probability for ATI.

V. RESULTS FOR TWO-COLOR PROCESSES: 285 AND 1064 nm

The ATI yield in the one-color experiment is rather low, due to the combination of the high photon energy and the relatively low intensity of the laser field. Enhancement of the intensity would increase the ATI yield since the ATI process has a higher order of nonlinearity than MPI. Also a reduction of the energy of the photon would help to increase the ATI yield, since continuum-continuum matrix elements are roughly proportional to ω^{-2}. Unfortunately neither approach can be used in a one-color experiment. As mentioned before, the high photon energy is required to overcome the substantial ionization potential of hydrogen with a reasonably low number of photons. The number of photons involved should be kept rather small, otherwise the resonance effects are completely washed out. For the same reason the intensity of the laser can not be increased. This would also lead to a reduction of the role of the resonances in the ionization process. The resonance effects are essential for the selection of the light intensity, by means of the Stark-shift tuning mechanism.

Therefore we turned to experiments with two laser beams of different colors, where the uv beam with the large photon energy is used to transfer the main part of the energy to the atomic electron, and a second color of high intensity (the fundamental of the YAG laser, 1.064 μm) is used to stimulate ATI and related processes. In order to use the Stark-shift tuning mechanism in a sensible way it is of course of major importance that the ac Stark shift is only caused by one of the two applied laser fields and is not a combined effect due to both fields. In the present experiment the Stark shift is uniquely determined by the infrared field, not only because the infrared field is much stronger than the uv field but also because the ac-Stark-shift coefficient is a factor of 30 larger for ir light than for uv light. Under these conditions the uv-wavelength detuning can be used to select the infrared intensity at which the process can take place. Addition of the Nd:YAG fundamental wavelength (1.064 μm) to the three-photon $3p$ resonant process indeed broadens the $3p$ resonance profile [Fig. 2(b)]. From the observed ac Stark shift, we derive an intensity of the infrared light of $\approx10^{11}$ $\mathrm{W/cm^2}$. Still this did not result in measurable two-photon ionization out of this state; we could easily have raised the infrared intensity, but then the process rate for ionization directly out of the ground state becomes appreciable, possibly with help of the uv beam. The reason for this is probably that the three-photon excitation step takes place only at the very highest intensities of the uv multimode pulse; under that condition it is difficult for the two-photon ir process to compete with the ionization out of $3p$ with a single uv photon.

In order to alleviate this problem, a process was studied in which the excitation step did not bias the ionization so much in favor of the uv light, namely with two uv and three ir photons to the $3p$ state: the notation also to be

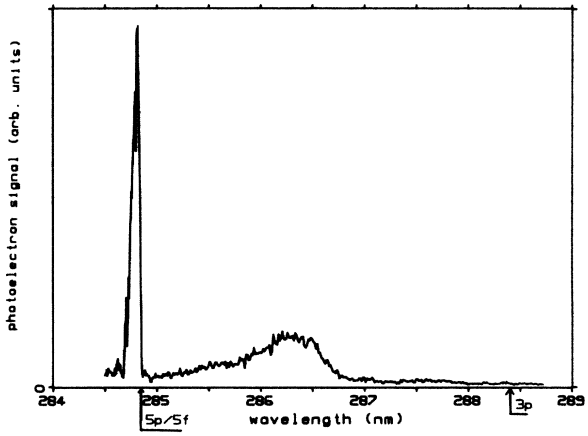

FIG. 7. The total ionization signal with 1.064 μm radiation present as a function of uv wavelength. The weak-field position of the $5p/5f$ (with three uv) and $3p$ (with two uv + three ir photons) are indicated.

TABLE IV. An overview of the peaks in the photoelectron spectra of Fig. 1.

Peak number in Fig. 1	Excitation process	Photoelectron energy (eV)	Possible resonance	At λ (nm)
1	$3\omega_1+\omega_2$	0.6	$5p/5f$	284.85
2	$2\omega_1+5\omega_2$	0.9	$3p$	288.45
3	$3\omega_1+2\omega_2$	1.7	$5p/5f$	284.85
4	$3\omega_1+3\omega_2$	2.9	$5p/5f$	284.85
5	$4\omega_1$	3.8	$5p/5f$	284.85

used in the remainder of this section, is $2\omega_1+3\omega_2$. A slightly different uv wavelength brings the electron in the $5p$ or $5f$ states (which in hydrogen are degenerate as far as our energy resolution is concerned), with a sequence of three uv photons. These $5p$ and $5f$ states are sufficiently close to the threshold to ionize with one ir photon. A uv-wavelength scan of the ionization signal (Fig. 7) shows the usual asymmetrically broadened $5p/5f$ resonance profile and a continuous background. At first glance the $3p$ resonance seems to be missing, and a very broad unidentified peak is present. At various wavelengths in this range the electron energy spectrum was also recorded (Fig. 1). The peaks in this figure have been numbered 1 to 5, and are listed together with their assignment in Table IV. This reveals that the broad resonance at 286.5 nm in the total ionization signal is due to electrons with an energy of 0.9 eV (peak No. 2 in Fig. 1). This indicates that they are formed by ionization with $(2\omega_1+5\omega_2)$, i.e., ionization with $2\omega_2$ from $3p$. Apparently the high infrared intensity required to induce a transition with so many photons shifts the resonance by a very large amount. The rate of ionization via this process is not only determined by the rate-limiting excitation step, but also by the competition between ionization with ω_1 and $2\omega_2$ from $3p$. We would therefore expect this rate to be fifth order in the infrared intensity (i.e., uv detuning), and this high order effectively suppresses the signal at small detunings. The infrared intensity needed to shift the $3p$ state by 3 nm is 2×10^{11} W/cm^2. Unfortunately even at these high intensities there is no evidence for the occurrence of ATI. The only peaks that have an energy compatible with ATI are the 1.7 eV electrons (peak No. 3 in Fig. 1) that are caused by ionization with $3\omega_1+2\omega_2$ photons. Note that ionization is already possible through a $(3\omega_1+1\omega_2)$ process, resulting in the 0.6-eV electron signal (peak No. 1). A complication with this kind of processes however, is that there are many sequences in which it is possible to stack the photons of different frequencies, each defining a certain pathway, which all interfere to produce the final result. Only the $(3\omega_1+n\omega_2)$ sequences that start with absorption of $3\omega_1$ are enhanced by the $5p$ resonance, but from a wavelength scan of the $3\omega_1+1\omega_2$ electron yield [Fig. 8(b)] it can be seen that a nonresonant contribution is also present. Part of this results from processes that absorb the photons in a different order, like $2\omega_1$ followed by $2\omega_2$ and then again ω_1. Pathways such as this have their virtual intermediate states in the region of the atomic spectrum that is croweded with real levels. This enhances the corresponding matrix elements as compared to the ATI pathways. In Table II matrix elements are shown for various pathways, supporting this interpretation. This explains why in Fig. 1(e) the $3\omega_1+2\omega_2$ peak can be larger than the $3\omega_1+1\omega_2$ peak: The former one has contributions from pathways that end with an ω_1 photon. Most of the intensity in the former peak comes from this type of pathways, and thus does not represent ATI at all.

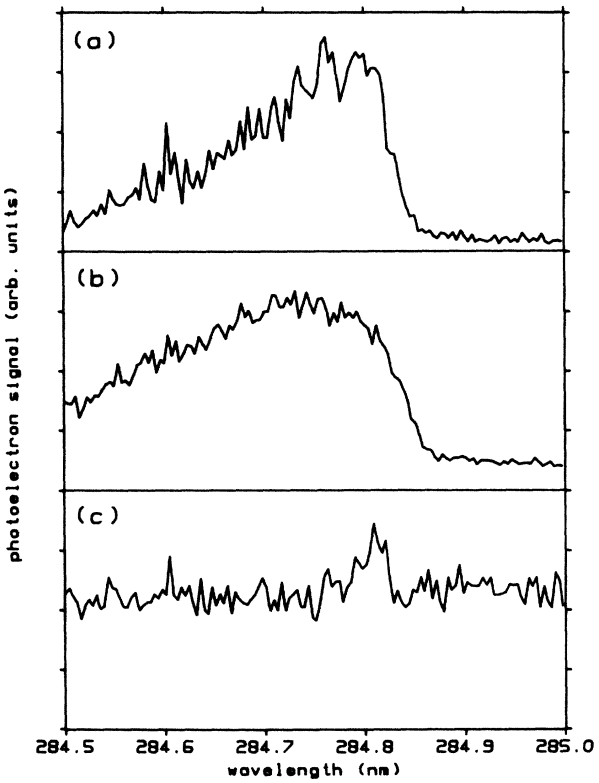

FIG. 8. Resonance profiles for $5p+5f$. (a) shows the production of 3.8-eV electrons by four uv photon ionization, (b) 0.6-eV electrons (three uv + ir), and (c) 1.75-eV electrons (three uv + two ir). The profile in (b) extends to shorter wavelength, because the higher ac-Stark shift needed to accomplish resonance there requires higher ir intensity, deciding the competition between ionization with uv and ir in favor of the latter. Note the nonresonant background of 0.6-eV electrons. Although some structure seems to be present in the 1.75-eV photoelectron yield, this does not reproduce well. Clearly almost all signal at this energy is due to nonresonant processes.

VI. CONCLUSIONS

Even though the yield is low, we have been able to demonstrate a method which reproduces the calculated ATI to within 10%. The low yield is mainly due to the high frequency of the light needed to overcome the rather large ionization potential of hydrogen with a reasonable number of photons. Attempts to perform the ionization with a low-frequency laser out of excited states prepared with a high-frequency laser suffer from two effects: One is the unfavorable branching ratios due to strong preference for the excitation step to occur when the high-frequency field is strong; the second is the many possible stacking orders of the different photons. This makes it impossible to speak of a certain peak as ATI, because ATI and non-ATI pathways all interfere to produce such a peak.

ACKNOWLEDGMENTS

This work is part of the research program of the Stichting voor Fundamenteel Onderzoek der Materie (Foundation for Fundamental Research on Matter) and was made possible by financial support from the Nederlandse Organisatie voor Zuiver-Wetenschappelijk Onderzoek (Netherlands Organization for Advancement of Pure Research).

[1]S. Chin and P. Lambropoulos, *Multiphoton Ionization of Atoms* (Academic, New York, 1984).

[2]M. J. van der Wiel and H. G. Muller, in *Abstracts of the Fourteenth International Conference on the Physics of Electronic and Atomic Collisions, Palo Alto, 1985,* edited by M. G. Coggiola, D. L. Huestis, and R. P. Saxon (ICPEAC, Palo Alto, 1985).

[3]M. Aymar and M. Crance, J. Phys. B **14**, 3585 (1981).

[4]G. Petite, F. Fabre, P. Agostini, M. Crance, and M. Aymar, Phys. Rev. A **29**, 2677 (1984).

[5]P. Kruit, H. G. Muller, J. Kimman, and M. J. van der Wiel, J. Phys. B **16**, 937 (1983).

[6]P. Kruit, W. R. Garrett, J. Kimman, and M. J. van der Wiel, J. Phys. B **16**, 3191 (1983).

[7]P. Kruit, H. G. Muller, J. Kimman, and M. J. van der Wiel, J. Phys. B **16**, 2359 (1983).

[8]A. Maquet, S.-I. Chu, and W. P. Reinhardt, Phys. Rev. A **27**, 2946 (1983).

[9]S.-I. Chu and J. Cooper, Phys. Rev. A **32**, 2769 (1985).

[10]D. E. Kelleher, M. Ligare, and L. R. Brewer, Phys. Rev. A **31**, 2747 (1985).

[11]S. Klarsfeld and A. Maquet, J. Phys. B **12**, L553 (1979).

[12]E. Karule, J. Phys. B **18**, 2207 (1985).

[13]M. Aymar and M. Crance, J. Phys. B **13**, L287 (1980).

[14]H. G. Muller (unpublished).

[15]H. G. Muller, H. B. van Linden van den Heuvell, and M. J. van der Wiel (unpublished).

[16]P. Kruit and F. H. Read, J. Phys. E **16**, 313 (1983).